HHS Public Access

Author manuscript

ACS Appl Mater Interfaces. Author manuscript; available in PMC 2018 February 24.

Published in final edited form as:

ACS Appl Mater Interfaces. 2018 January 24; 10(3): 2275–2281. doi:10.1021/acsami.7b12145.

Bacterial Adhesion Is Affected by the Thickness and Stiffness of Poly(ethylene glycol) Hydrogels

Kristopher W. Kolewe[1], **Jiaxin Zhu**[2], **Natalie R. Mako**[1], **Stephen S. Nonnenmann**[2], and **Jessica D. Schiffman**[1,*]

[1]Department of Chemical Engineering, University of Massachusetts Amherst, Amherst, Massachusetts 01003-9303

[2]Department of Mechanical and Industrial Engineering, University of Massachusetts Amherst, Amherst, Massachusetts 01003-9265

Abstract

Despite lacking visual, auditory, and olfactory perception, bacteria sense and attach to surfaces. Many factors including, the chemistry, topography, and mechanical properties of a surface, are known to alter bacterial attachment, and in this study, using a library of nine protein-resistant poly(ethylene glycol) (PEG) hydrogels immobilized on glass slides, we demonstrate that the thickness or amount of polymer concentration also matters. Hydrated atomic force microscopy and rheological measurements corroborated that thin (15 μm), medium (40 μm), and thick (150 μm) PEG hydrogels possessed Young's moduli in three distinct regimes, soft (20 kPa), intermediate (300 kPa), and stiff (1000 kPa). The attachment of two diverse bacteria, flagellated gram-negative *Escherichia coli* and non-motile gram-positive *Staphylococcus aureus* was assessed after a 24 h incubation on the nine PEG hydrogels. On the thickest PEG hydrogels (150 μm), *E. coli* and *S. aureus* attachment increased with increasing hydrogel stiffness. However, when hydrogel's thickness was reduced to 15 μm, a substantially greater adhesion of *E. coli* and *S. aureus* was observed. Twelve times fewer *S. aureus* and eight times fewer *E. coli* adhered to thin-soft hydrogels than to thick-soft hydrogels. Though a full mechanism to explain this behavior is beyond the scope of this paper, we suggest that because the Young's moduli of thin-soft and thick-soft hydrogels were statistically equivalent, potentially, the very stiff underlying glass slide was causing the thin-soft hydrogels to feel stiffer to the bacteria. These findings suggest a key takeaway design rule; to optimize fouling-resistance, hydrogel coatings should be thick and soft.

TOC image

*Corresponding Authors: schiffman@ecs.umass.edu.

Supporting Information. The Supporting Information is available free of charge on the ACS Publications website. Figure S1 provides AFM topographical images of dried hydrogels. Figure S2 provides AFM topographical images of hydrated hydrogels. Table S1 provides average surface roughness values for the hydrated PEG hydrogels. Table S2 provides properties of PEG hydrogels. Figure S3 provides representative micrographs of *S. aureus* adhesion to hydrogels. Figure S4 provides representative micrographs of *E. coli* adhesion to hydrogels.

Keywords

Antifouling; Atomic Force Microscopy; Hydrogel; Poly(ethylene glycol); *Escherichia coli*; *Staphylococcus aureus*

INTRODUCTION

In nature, 99% of bacteria are part of robust complex biological systems attached to surfaces.[1–3] Hence, bacterial communities present on the engineered surfaces found in food industries, maritime operations, and biotechnology remain challenging to eliminate.[4–7] Much research has focused on optimizing the chemistry and surface energy of materials to minimize the non-specific adsorption of proteins and biomacromolecules, which facilitates microbial adhesion and biofilm formation.[8–11] Many other factors influence the attachment of microorganisms to surfaces, including roughness[12–14] and topography.[15,16] Moreover, an emerging body of evidence suggests that the stiffness of a substrate also affects bacterial attachment.[1–3,17–22]

Previous studies conducted on ultrathin (~50 nm) poly(allylamine hydrochloride) and poly(acrylic acid) polyelectrolyte multilayered films showed that more *Escherichia coli* (*E. coli*) and *Staphylococcus epidermis* attached to their stiffest films, 100,000 kPa versus their softest films, 1,000 kPa.[17] Recently, we demonstrated that independent of hydrogel chemistry and incubation time, the adhesion of both *E. coli* and *Staphylococcus aureus* (*S. aureus*) scaled linearly with stiffness on thick (150 μm) poly(ethylene glycol) dimethacrylate (PEG) and agar hydrogels that ranged from 44 kPa to 6500 kPa.[18] Guégan *et al.* determined that a greater adhesion of *Pseudoalteromonas sp.* D41 occurred on agarose hydrogels that had a storage modulus of 110 kPa than on soft agarose hydrogels that had a storage modulus of 6.6 kPa.[23] Additionally, proteomic profiling indicated that significant phenotypic changes (i.e., differential regulation of key metabolic pathways and an increased synthesis of outer membrane proteins) occurred to the bacteria that adhered to the stiffer versus the softer agarose hydrogels. These studies definitively show that bacteria respond to substrate stiffness or polymer concentration and exhibit phenotypic changes in response to surface association.[24] However, if this stiffness preference depends on hydrogel thickness remains an open question.

Here, for the first time, we systematically control the thickness and stiffness of hydrogels to decouple their effects on bacterial adhesion, Figure 1. We selected the antifouling polymer, PEG, as our model hydrogel system because of its excellent protein fouling resistance.[25,26] To ensure that PEG hydrogels of various thicknesses (15 μm, 40 μm, and 150 μm) were synthesized with three distinct thickness-independent Young's moduli (~20, ~300, and

~1000 kPa) we performed local nanomechanical characterization using atomic force microscopy (AFM) in an aqueous environment. Hydrated AFM is the optimal technique to study the local mechanical properties of fully hydrated soft hydrogels[27] since it does not introduce artifacts typically observed with scanning electron microscopy or dry AFM.[28–32] Because of their unique surface sensing mechanisms,[33,34] bacteria adhesion studies were conducted using two model microbes, non-motile gram-positive *S. aureus* and flagellated gram-negative *E. coli*. By combining well-controlled PEG hydrogel design parameters (antifouling chemistry, thickness, stiffness) with two distinct model bacteria we have formed a powerful platform to systematically evaluate if bacteria adhesion is affected by the thickness or amount of PEG concentration in a hydrogel coating.

MATERIALS AND METHODS

Materials

All compounds were used as received. Poly(ethylene glycol) dimethacrylate, (PEG, M_n = 750 Da), 3-(trimethoxysilyl)propyl methacrylate, phosphate buffered saline (PBS, 10× sterile biograde) were purchased from Sigma-Aldrich (St. Louis, MO). Irgacure 2959 was obtained from BASF (Ludwigshafen, Germany). Deionized (DI) water was obtained from a Barnstead Nanopure Infinity water purification system (Thermo Fisher Scientific, Waltham, MA).

Hydrogel Fabrication

PEG solutions (10, 25, and 50 vol% in 162.7 mM PBS, corresponding to soft, intermediate and stiff hydogels) were sterile filtered using a 0.2 μm syringe, then degassed using nitrogen gas. For UV-curing, 0.8 wt% Irgacure 2959 (a radical photo initiator) was added to the PEG solution with induction under a long wave UV light, 365 nm for 10 min. Hydrogels with three different thicknesses (thin, medium, and thick) were prepared by depositing 10, 40, and 85 μL aliquots of a PEG solution onto a glass coverslip (22-mm Fisher Scientific) that was functionalized with 3-(trimethoxysilyl)propyl methacylate.[35] A clean 22-mm coverslip was placed on top of the PEG solution to limit oxygen diffusion, facilitate polymerization, and to enable a uniform hydrogel thickness. Following polymerization, the top coverslip was removed using forceps and the PEG hydrogels immobilized on glass slides were swollen for 48 hr in 162.7 mM PBS.

Hydrogel Characterization

The thickness of PEG hydrogels was determined using a digital micrometer (Mitutoyo Corporation, Kawaski, Japan) by averaging 5 measurements on at least 3 fully swollen hydrogels. Surface topographic images of hydrogels were acquired using a Cypher ES atomic force microscope (AFM, Asylum Research/Oxford Instruments, Goleta, CA). Dry hydrogels were imaged in AC mode in air using Tap300-G cantilevers (Budget Sensors, Watsonville, CA) while hydrated hydrogels were imaged using a closed perfusion cell in water AC mode using Olympus TR800PSA (k = 183.54 pN/nm) cantilevers. The topographical profiles were analyzed using Igor Pro 6.37 (WaveMetrics, Inc., Lake Oswego, OR) to quantify the surface roughness of the hydrated hydrogels, including, their route mean square roughness (R_q), average roughness (R_a), skewness (R_{shw}), kurtosis (R_{kur}) minimum

roughness (R_{min}), and maximum roughness (R_{max}).[36] The local stiffness of hydrogels was obtained using TR400PB cantilevers through AFM nanoindentation in water at 3 distinct locations on each of 9 fully swollen hydrogels. Thermal calibration in air was first performed to determine the probe's spring constant (k = 29.56 pN/nm). Subsequently, a calibration force curve on a hard surface (silicon) in water was obtained using same probe to determine the lever sensitivity (Invols = 36.34 nm/V). Considering the cone shape of the chosen AFM tip, the Young's moduli was determined by data analysis in Igor Pro using the Sneddon's model:[37]

$$F=\frac{\pi}{2}\times\frac{E}{1-\upsilon^2}\times\tan\alpha\times\delta^2 \quad \text{Equation 1}$$

where $F, E, \upsilon, \alpha, \delta$ are the applied force, the reduced modulus, sample's Poisson ratio, half-opening angle of AFM tip and depth of indentation.

The bulk mechanical properties of PEG hydrogels were determined through small amplitude oscillatory shear measurements using a plate–plate geometry (Kinexus Pro rheometer (Malvern Instruments, UK), with a diameter of 20 mm and a gap of 1 mm. All hydrogels were prepared for rheology using 1 mm deep Teflon molds that had a 25-mm diameter; hydrogels were loaded into the rheometer and then trimmed to size using a razor blade. A strain amplitude sweep was performed to ensure that experiments were conducted within the linear viscoelastic region and a strain percent of 0.1% was selected. Oscillation frequency sweeps were conducted over an angular frequency domain, 1.0 and 100 rad/s at 23 °C. As hydrogels are incompressible solids with a Poisson ratio of 0.5, the Young's modulus was calculated from the complex modulus using the Trouton ratio, Equation 2[38]:

$$E=2G^*(1-\upsilon) \quad \text{Equation 2}$$

where E, G^*, and v are the Young's modulus, complex modulus, and the sample's Poisson ratio.

Evaluation of Bacterial Growth

E. coli K12 MG1655 was purchased from DSMZ (Leibniz-Institut, Germany) and transformed with pMF230, a high copy GFP plasmid. *S. aureus* SH1000 containing the high-efficiency sGFP was a generous donation of Dr. Alexander Horswill (University of Colorado Anschutz Medical Campus). Hydrogels immobilized on glass slides were placed at the base of 6-well polystyrene plates (Fisher Scientific) to which 5 mL of M9 media containing 100 μg/mL ampicillin or 10 μg/mL chloramphenicol was added for *E. coli* or *S. aureus* (1.00×10^8 cells/mL), respectively. Internal controls (glass coverslips) were run in parallel (data not shown). The growth media in each well was inoculated with an overnight culture of *E. coli* or *S. aureus*, which were washed and resuspended in M9 media,[18,39] before being placed in an incubator at 37 °C for 24 hr. Hydrogels with attached bacteria were removed from the 6-well polystyrene plates and washed with PBS to remove loosely adhered bacteria. *E. coli* and *S. aureus* attachment was evaluated using an adhesion

assay[40,41] that monitored the bacteria colony coverage within a 366,964 μm^2 area using a Zeiss Microscope Axio Imager A2M (20× magnification, Thornwood, NY). The particle analysis function in *ImageJ 1.48* software (National Institutes of Health, Bethesda, MD) was used to calculate the bacteria colony area coverage (%) by analyzing 10–15 randomly acquired images over three parallel replicates. Significant differences between samples were determined with an unpaired student *t*-test. Significance ($p \leq 0.05$) is denoted in graphs using asterisks.

RESULTS AND DISCUSSION

Characteristics of PEG Hydrogels

By controlling the volume of poly (ethylene glycol) dimethacrylate (PEG) solution deposited onto glass slides, we have successfully synthesized hydrogels with three distinct thicknesses, Figure 1. A digital micrometer was used to determine that the average thickness of the thin hydrogels was 14 ± 2 μm, the medium hydrogels was 49 ± 4 μm, and the thick hydrogels was 155 ± 8 μm thick. Because all of the hydrogels are comprised of the same PEG chemistry, they displayed excellent resistivity to the adsorption of serum proteins, consistent with previous reports.[18]

The Young's modulus of the hydrogels was tuned by increasing the polymer concentration. While rheology is commonly used to characterize the mechanical properties of very thick hydrogels (1000 μm), we needed to confirm that decreasing the thickness of the hydrogels did not change their Young's moduli. Therefore, we characterized the mechanical properties of our hydrogels using hydrated atomic force microscopy (AFM). To validate our AFM approach, we acquired topographic images of PEG hydrogels that were dried at room temperature (Figure S1) and compared them to hydrogels that were maintained in an aqueous environment (Figure S2). While the dried hydrogels appeared wrinkled, collapsed, and decorated with salt precipitates,[28] by maintaining hydration during analysis, the surfaces were smooth and extensive analysis of the surface roughness demonstrated that there was no correlation between the surface roughness and thickness of hydrogels, Table S1[41,42] Notably, there was no discernable trend between the thickness of the hydrogels and their route mean square roughness (R_q), average roughness (R_a), skewness (R_{shw}), kurtosis (R_{kur}) minimum roughness (R_{min}), or maximum roughness (R_{max}). With an optimized method for keeping the hydrogels hydrated, we next confidently characterized the Young's moduli of the hydrogels.

Figure 2 and Table S2 contain the Young's modulus of thin, medium, thick hydrogels acquired using hydrated AFM, as well as the bulk rheological measurements acquired on very thick (1000 μm) hydrogels. AFM determined that the thin-stiff, medium-stiff, and thick-stiff hydrogels had a statistically equivalent Young's modulus values of 950 ± 90 kPa, 1000 ± 90 kPa, and 11000 ± 90 kPa, respectively, which were consistent with the literature.[27,43] There was no statistical differences between the two techniques; the Young's moduli of soft and intermediate hydrogels at all thicknesses (thin, medium, thick, and bulk) was the same. While the AFM measurements were consistent within the stiff hydrogels (thin, medium, and thick), their Young's moduli were lower than that acquired using rheology. This was likely because the lower water content of the stiff hydrogels exacerbated the

differences between the compressive AFM measurements and shear rheological measurements, as previously reported.[44] The reasonable agreement between local and bulk measurements reaffirms that polymer concentration dictates mechanical properties of the PEG hydrogels and allows us to group the thin, medium, and thick hydrogels into three distinct regimes based on their Young's modulus: soft, intermediate and stiff.

General Trends Regarding the Attachment of *S. aureus* and *E. coli* to PEG Hydrogels

Consistent with literature,[9,45] the presence of any hydrophilic PEG coating statistically reduced the amount of adhered bacteria compared to internal glass controls by ~95% for *S. aureus* and by ~93% for *E. coli*. Despite the reduction, it is notable that some microbes still attach and this study investigates how microbial attachment is affected by the thickness and stiffness of a PEG hydrogel layer. To decouple the effect that hydrogel stiffness and thickness pose on bacterial adhesion, we conducted static bacterial adhesion experiments in minimal growth media on thin, medium, and thick PEG hydrogels (immobilized on glass slides), which were fabricated at each stiffness regime (Figure 1). Two general trends emerged following a 24 h incubation: (1) fewer bacteria adhered to soft hydrogels than to stiff hydrogels and (2) more bacteria adhered to thin hydrogels than to thick hydrogels at all stiffnesses. Due to the substantial differences in the data, which likely resulted from unique sensing and/or attachment mechanisms, the specific results for each bacterium is discussed separately.

Attachment of *S. aureus* to PEG Hydrogels

Representative fluorescent micrographs of *S. aureus* incubated on PEG hydrogels are provided in Figure S3. Consistent with our previous study on thick PEG hydrogels,[18] *S. aureus* adhesion scaled with stiffness, as demonstrated by the statistically significant higher colony coverage on intermediate and stiff hydrogels (15 times and 25 times, respectively) than on the soft hydrogels, Figure 3. For the thin (15 μm) hydrogels, the effect of stiffness was significantly diminished, where the colony area coverage of *S. aureus* on thin-intermediate and thin-stiff hydrogels was 1.2 and 2 times greater than on the thin-soft hydrogels. Interestingly, the thickness of intermediate and stiff hydrogels had no impact on *S. aureus* adhesion, as the thin-intermediate, medium-intermediate, and thick-intermediate hydrogels induced statistically equivalent surface coverages of 2.5 ± 0.4%, 2.4 ± 0.3%, and 2.7 ± 0.2%, respectively. The thickness of soft hydrogels, which were immobilized on glass slides, however, displayed a profound effect on *S. aureus* adhesion. Significantly more bacteria adhered to thin-soft hydrogels than thick-soft hydrogels (99% confidence). There were statistically different area coverages of 1.9 ± 0.2%, 1.3 ± 0.5%, and 0.4 ± 0.2% on thin-soft, medium-soft, and thick-soft hydrogels, respectively. These results suggest that *S. aureus* surface attachment is sensitive to the thickness of soft hydrogels.

Attachment of *E. coli* to PEG Hydrogels

Hydrogel thickness had a greater effect on *E. coli* adhesion than *S. aureus* adhesion. Consistent with our previous study,[18] more *E. coli* adhered to thick-stiff hydrogels than to thick-soft hydrogels, with 4 times and 7 times more colony coverage observed on the thick-intermediate and thick-stiff hydrogels than on the thick-soft hydrogels, respectively (Figure 4). Notably the area coverage of *E. coli* on the thick hydrogels was statistically lower than

the *E. coli* coverage on thin and medium thickness hydrogels across all three stiffness regimes. Thin-stiff and medium-stiff hydrogels displayed a statistically equivalent *E. coli* coverage of 3.0 ± 0.4% and 2.9 ± 0.1%, respectively, but significantly less adhesion (95% confidence) than the thick-stiff hydrogels, 2.2 ± 0.2%. The *E. coli* adhesion on thin hydrogels occurred independent of stiffness, 1.9 ± 0.3%, 2.3 ± 0.5%, and 3.0 ± 0.4% for the thin-soft, thin-intermediate, and thin-stiff hydrogels, respectively.

Discussion and Implications on Designing Antifouling Coatings

Our results demonstrate that two different bacteria, non-motile gram-positive *S. aureus* and flagellated gram-negative *E. coli*, adhered to PEG hydrogels in distinct manners, as evident by their different thickness and stiffness dependencies. The heat maps shown in Figure 5 displays the relative adhesion of *E. coli* and *S. aureus* as a function of hydrogel thickness and Young's modulus, thus facilitating a direct comparison of structure-property relationships between the two-microbial species. For example, the *E. coli* adhesion dependence observed on the intermediate hydrogels is noticeably absent from *S. aureus*, indicative of a species-specific phenotype. The remarkably similar increase in bacterial adhesion observed for both species on the soft hydrogels suggests that for soft hydrogels, the thickness of that hydrogel coating matters. We hypothesize that both bacteria types feel through the thin hydrogels sensing the underlying very stiff glass substrate, thus instigating increased adhesion typical of a stiffer material. Notably, the hydrogels used in this study are comprised of the same protein-resistant PEG chemistry and consistent surface roughness. However, surface features arising from hydrogel formation including local polymer fluctuations or the release of air bubbles can create topographical features than may cause bacteria to view the hydrogels differently. Bacteria lack visual, auditory, and olfactory perception; surface sensing by bacteria is considered to occur as a combination of chemical signaling cues and physical appendage or membrane-based interactions.[34] After adhering to a surface, the membrane of a microbe deforms, which causes the bacteria to react to the membrane stress and change from a planktonic to a biofilm phenotype.[46] The mechanisms controlling the adhesion of bacteria to surfaces and the deformation of the cell membrane have been well studied on metal and polymeric materials.[47–49]

The extracellular organelle of *E. coli* are known to probe the stiffness of a surface in a manner similar to an AFM cantilever.[33,50] Unlike *E. coli*, *S. aureus* lacks extracellular appendages, thus an alternative surface sensing mechanism must dictate the statistically different adhesive behavior of *S. aureus*. While the mechanism remains unknown,[51] Li *et al.* reported that the kinetics of *S. aureus* adhesion was altered by shear stress, but does not alter *S. aureus'* expression of fibronectin-binding or collagen-binding proteins.[52] In this study, membrane deformation potentially plays a role due to the difference in Young's moduli between the peptidoglycan membrane of *S. aureus* and the hydrogel's stiffness. AFM force spectroscopy studies previously determined that the Young's modulus of the peptidoglycan membrane of *S. aureus* was ~ 47 kPa,[53] comparable to the soft hydrogels used in this study, but significantly less than the intermediate and stiff hydrogels. Thus, soft hydrogels would deform more upon *S. aureus* contact, potentially enhancing the sensing mechanism and subsequently increasing the likelihood of adhesion. While the exact mechanism of how or why individual microbes display depth sensitivity is beyond the scope of this manuscript, we

suggest that antifouling coatings should be designed with thickness in mind and that these results will spur further study in the burgeoning field of microbial response to substrate mechanics.

CONCLUSION

To our knowledge, this is the first demonstration that bacterial attachment displays a depth-sensitivity through hydrogels to an underlying stiff substrate. Through systematic, AFM characterization under aqueous environments, we decoupled hydrogel stiffness and thickness effects on the depth sensing of two diverse microbial species, *S. aureus* and *E. coli*. Decreasing the thickness of PEG hydrogels significantly increased bacterial adhesion, as 12 times more *S. aureus* and 8 times more *E. coli* adhered to the thin-soft hydrogels than to the thick-soft hydrogels. *S. aureus* adhesion was strongly influenced by the thickness of soft hydrogels, but displayed only minimal variation in bacterial adhesion on thinner intermediate and stiff hydrogels. *E. coli* displayed greater thickness-dependence; a higher colony coverage occurred on medium than on thick hydrogels of all Young's moduli. The substantial differences in bacterial adhesion observed between thin and thick hydrogels suggests that the underlying stiff substrate may have influenced the perceived mechanical properties of the hydrogel by the adherent bacteria. These findings suggest that bacteria are sensitive to the thickness of soft hydrogels.

Supplementary Material

Refer to Web version on PubMed Central for supplementary material.

Acknowledgments

KWK was supported by National Research Service Award T32 GM008515 from the National Institutes of Health. This work was partially supported by the Professor James M. Douglas Career Development Faculty Award and the Armstrong Fund for Science.

References

1. Hall-Stoodley L, Costerton JW, Stoodley P. Bacterial Biofilms: From the Natural Environment to Infectious Diseases. Nat Rev Microbiol. 2004; 2:95–108. [PubMed: 15040259]
2. Flemming HC, Wingender J, Szewzyk U, Steinberg P, Rice SA, Kjelleberg S. Biofilms: An Emergent Form of Bacterial Life. Nat Rev Microbiol. 2016; 14:563–575. [PubMed: 27510863]
3. Nadell CD, Drescher K, Foster KR. Spatial Structure, Cooperation and Competition in Biofilms. Nat Rev Microbiol. 2016; 14:589–600. [PubMed: 27452230]
4. Costerton JW, Stewart PS, Greenberg EP. Bacterial Biofilms: A Common Cause of Persistent Infections. Science. 1999; 284:1318–1322. [PubMed: 10334980]
5. Chmielewski RAN, Frank JF. Biofilm Formation and Control in Food Processing Facilities. Compr Rev Food Sci Food Saf. 2003; 2:22–32.
6. Schultz MP, Bendick JA, Holm ER, Hertel WM. Economic Impact of Biofouling on a Naval Surface Ship. Biofouling. 2011; 27:87–98. [PubMed: 21161774]
7. Callow JA, Callow ME. Trends in the Development of Environmentally Friendly Fouling-Resistant Marine Coatings. Nat Commun. 2011; 2:244. [PubMed: 21427715]
8. Darouiche RO, Weinstein RA. Device-Associated Infections: A Macroproblem That Starts with Microadherence. Clin Infect Dis. 2001; 33:1567–1572. [PubMed: 11577378]

9. Banerjee I, Pangule RC, Kane RS. Antifouling Coatings: Recent Developments in the Design of Surfaces That Prevent Fouling by Proteins, Bacteria, and Marine Organisms. Adv Mater. 2011; 23:690–718. [PubMed: 20886559]
10. Ratner BD, Bryant SJ. Biomaterials: Where We Have Been and Where We Are Going. Annu Rev Biomed Eng. 2004; 6:41–75. [PubMed: 15255762]
11. Ista, Linnea K., Callow, Maureen E., Finlay, John A., Coleman, Sarah E., Nolasco, Aleece C., Simons, Robin H., Callow, James A., Lopez, GP. Effect of Substratum Surface Chemistry and Surface Energy on Attachment of Marine Bacteria and Algal Spores Effect of Substratum Surface Chemistry and Surface Energy on Attachment of Marine Bacteria and Algal Spores. Appl Environ Microbiol. 2004; 70:4151–4157. [PubMed: 15240295]
12. An YH, Friedman RJ. Concise Review of Mechanisms of Bacterial Adhesion to Biomaterial Surfaces. J Biomed Mater Res. 1998; 43:338–348. [PubMed: 9730073]
13. Katsikogianni M, Missirlis YF. Concise Review of Mechanisms of Bacterial Adhesion to Biomaterials and of Techniques Used in Estimating Bacteria-Material Interactions. Eur Cell Mater. 2004; 8:37–57. [PubMed: 15593018]
14. Bazaka K, Crawford RJ, Ivanova EP. Do Bacteria Differentiate between Degrees of Nanoscale Surface Roughness? Biotechnol J. 2011; 6:1103–1114. [PubMed: 21910258]
15. Dobosz KM, Kolewe KW, Schiffman JD. Green Materials Science and Engineering Reduces Biofouling: Approaches for Medical and Membrane-Based Technologies. Front Microbiol. 2015; 6:1–8. [PubMed: 25653648]
16. Perera-Costa D, Bruque JM, González-Martín ML, Gómez-García AC, Vadillo-Rodríguez V. Studying the Influence of Surface Topography on Bacterial Adhesion Using Spatially Organized Microtopographic Surface Patterns. Langmuir. 2014; 30:4633–4641. [PubMed: 24697600]
17. Lichter JA, Thompson MT, Delgadillo M, Nishikawa T, Rubner MF, Van Vliet KJ. Substrata Mechanical Stiffness Can Regulate Adhesion of Viable Bacteria. Biomacromolecules. 2008; 9:1571–1578. [PubMed: 18452330]
18. Kolewe K, Peyton SR, Schiffman JD. Fewer Bacteria Adhere to Softer Hydrogels. ACS Appl Mater Interfaces. 2015; 7:19562–19569. [PubMed: 26291308]
19. Persat A, Nadell CD, Kim MK, Ingremeau F, Siryaporn A, Drescher K, Wingreen NS, Bassler BL, Gitai Z, Stone HA. The Mechanical World of Bacteria. Cell. 2015; 161:988–997. [PubMed: 26000479]
20. Lee CK, Kim AJ, Santos GS, Lai PY, Lee SY, Qiao DF, De Anda J, Young TD, Chen Y, Rowe AR, Nealson KH, Weiss PS, Wong GCL. Evolution of Cell Size Homeostasis and Growth Rate Diversity during Initial Surface Colonization of Shewanella Oneidensis. ACS Nano. 2016; 10:9183–9192.
21. Persat A, Inclan YF, Engel JN, Stone HA, Gitai Z. Type IV Pili Mechanochemically Regulate Virulence Factors in Pseudomonas aeruginosa. Proc Natl Acad Sci U S A. 2015; 112:7563–7568. [PubMed: 26041805]
22. Song F, Ren D. Stiffness of Cross-Linked Poly(dimethylsiloxane) Affects Bacterial Adhesion and Antibiotic Susceptibility of Attached Cells. Langmuir. 2014; 30:10354–10362. [PubMed: 25117376]
23. Guégan C, Garderes J, Le Pennec G, Gaillard F, Fay F, Linossier I, Herry JM, Fontaine MNB, Réhel KV. Alteration of Bacterial Adhesion Induced by the Substrate Stiffness. Colloids Surfaces B Biointerfaces. 2014; 114:193–200. [PubMed: 24189194]
24. Sauer K, Camper AK. Characterization of Phenotypic Changes in Pseudomonas putida in Response to Surface-Associated Growth Characterization of Phenotypic Changes in Pseudomonas Putida in Response to Surface-Associated Growth. J Bacteriol. 2001; 183:6579–6589. [PubMed: 11673428]
25. Herrwerth S, Eck W, Reinhardt S, Grunze M. Factors That Determine the Protein Resistance of Oligoether Self-Assembled Monolayers - Internal Hydrophilicity, Terminal Hydrophilicity, and Lateral Packing Density. J Am Chem Soc. 2003; 125:9359–9366. [PubMed: 12889964]
26. Krishnan S, Weinman CJ, Ober CK. Advances in Polymers for Anti-Biofouling Surfaces. J Mater Chem. 2008; 18:3405–3413.

27. Galluzzi M, Biswas CS, Wu Y, Wang Q, Du B, Stadler FJ. Space-Resolved Quantitative Mechanical Measurements of Soft and Supersoft Materials by Atomic Force Microscopy. NPG Asia Mater. 2016; 8:e327.
28. González-Méijome JM, López-Alemany A, Almeida JB, Parafita MA, Refojo MF. Microscopic Observation of Unworn Siloxane-Hydrogel Soft Contact Lenses by Atomic Force Microscopy. J Biomed Mater Res - Part B Appl Biomater. 2006; 76:412–418. [PubMed: 16184533]
29. Kim SH, Opdahl A, Marmo C, Somorjai GA. AFM and SFG Studies of pHEMA-Based Hydrogel Contact Lens Surfaces in Saline Solution: Adhesion, Friction, and the Presence of Non-Crosslinked Polymer Chains at the Surface. Biomaterials. 2002; 23:1657–1666. [PubMed: 11922469]
30. Lira M, Santos L, Azeredo J, Yebra-Pimentel E, Real Oliveira MECD. Comparative Study of Silicone-Hydrogel Contact Lenses Surfaces before and after Wear Using Atomic Force Microscopy. J Biomed Mater Res - Part B Appl Biomater. 2008; 85:361–367. [PubMed: 17957701]
31. Barbucci R, Pasqui D, Favaloro R, Panariello G. A Thixotropic Hydrogel from Chemically Cross-Linked Guar Gum: Synthesis, Characterization and Rheological Behaviour. Carbohydr Res. 2008; 343:3058–3065. [PubMed: 18822410]
32. Tronci G, Grant CA, Thomson NH, Russell SJ, Wood DJ. Multi-Scale Mechanical Characterization of Highly Swollen Photo-Activated Collagen Hydrogels. J R Soc Interface. 2015; 12:20141079. [PubMed: 25411409]
33. Belas R. Biofilms, Flagella, and Mechanosensing of Surfaces by Bacteria. Trends Microbiol. 2014; 22:1–11. [PubMed: 24246882]
34. O'Toole GA, Wong GCL. Sensational Biofilms: Surface Sensing in Bacteria. Curr Opin Microbiol. 2016; 30:139–146. [PubMed: 26968016]
35. Liu VA, Bhatia SN. Three-Dimensional Patterning of Hydrogels Containing Living Cells. Biomed Microdevices. 2002; 4:257–266.
36. Truong VK, Lapovok R, Estrin YS, Rundell S, Wang JY, Fluke CJ, Crawford RJ, Ivanova EP. The Influence of Nano-Scale Surface Roughness on Bacterial Adhesion to Ultrafine-Grained Titanium. Biomaterials. 2010; 31:3674–3683. [PubMed: 20163851]
37. Sneddon IN. The Relation between Load and Penetration in the Axisymmetric Boussinesq Problem for a Punch of Arbitrary Profile. Int J Eng Sci. 1965; 3:47–57.
38. Trouton FT. On the Coefficient of Viscous Traction and Its Relation to that of Viscosity. Proc R Soc London. 1906; 77:426–440.
39. Zodrow KR, Schiffman JD, Elimelech M. Biodegradable Polymer (PLGA) Coatings Featuring Cinnamaldehyde and Carvacrol Mitigate Biofilm Formation. Langmuir. 2012; 28:13993–13999. [PubMed: 22937881]
40. Fux CA, Wilson S, Stoodley P. Detachment Characteristics and Oxacillin Resistance of Staphoccocus aureus Biofilm Emboli in an In Vitro Catheter Infection Model. J Bacteriol. 2004; 186:4486–4491. [PubMed: 15231780]
41. Chung KK, Schumacher JF, Sampson EM, Burne RA, Antonelli PJ, Brennan AB. Impact of Engineered Surface Microtopography on Biofilm Formation of Staphylococcus aureus. Biointerphases. 2007; 2:89–94. [PubMed: 20408641]
42. Drira Z, Yadavalli VK. Nanomechanical Measurements of Polyethylene Glycol Hydrogels Using Atomic Force Microscopy. J Mech Behav Biomed Mater. 2013; 18:20–28. [PubMed: 23237877]
43. Costa KD, Yin FC. Analysis of Indentation: Implications for Measuring Mechanical Properties with Atomic Force Microscopy. J Biomech Eng. 1999; 121:462–471. [PubMed: 10529912]
44. Stammen JA, Williams S, Ku DN, Guldberg RE. Mechanical Properties of a Novel PVA Hydrogel in Shear and Unconfined Compression. Biomaterials. 2001; 22:799–806. [PubMed: 11246948]
45. Hucknall A, Rangarajan S, Chilkoti A. In Pursuit of Zero: Polymer Brushes That Resist the Adsorption of Proteins. Adv Mater. 2009; 21:2441–2446.
46. Busscher HJ, van der Mei HC. How Do Bacteria Know They Are on a Surface and Regulate Their Response to an Adhering State? PLoS Pathog. 2012; 8:1–3.

47. Bos R, Van Der Mei HC, Busscher HJ. Physico-Chemistry of Initial Microbial Adhesive Interactions - Its Mechanisms and Methods for Study. FEMS Microbiol Rev. 1999; 23:179–229. [PubMed: 10234844]

48. Tuson HH, Weibel DB. Bacteria–Surface Interactions. Soft Matter. 2013; 9:4368–4380. [PubMed: 23930134]

49. Anselme K, Davidson P, Popa AM, Giazzon M, Liley M, Ploux L. The Interaction of Cells and Bacteria with Surfaces Structured at the Nanometre Scale. Acta Biomater. 2010; 6:3824–3846. [PubMed: 20371386]

50. Iscla I, Wray R, Blount P. The Oligomeric State of the Truncated Mechanosensitive Channel of Large Conductance Shows No Variance in Vivo. Protein Sci. 2011; 20:1638–1642. [PubMed: 21739498]

51. Li ZJ, Mohamed N, Ross JM. Shear Stress Affects the Kinetics of Staphylococcus aureus Adhesion to Collagen. Biotechnol Prog. 2000; 16:1086–1090. [PubMed: 11101338]

52. Islam N, Kim Y, Ross JM, Marten MR. Proteomic Analysis of Staphylococcus aureus Biofilm Cells Grown under Physiologically Relevant Fluid Shear Stress Conditions. Proteome Sci. 2014; 12:21. [PubMed: 24855455]

53. Chen Y, Norde W, Van Der Mei HC, Busscher HJ. Bacterial Cell Surface Deformation under External Loading. MBio. 2012; 3:1–7.

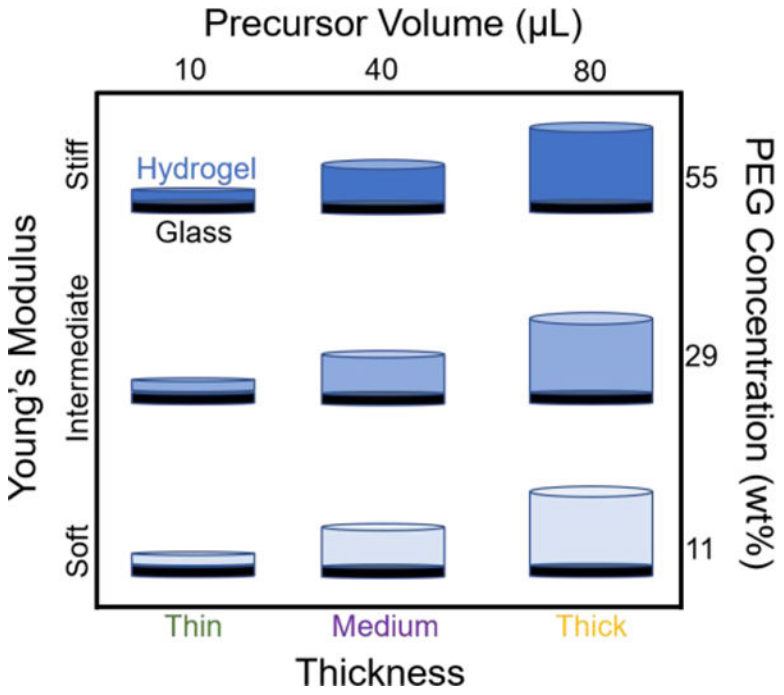

Figure 1.

A schematic of the nine PEG hydrogels tested in this study. Throughout the results section, we will refer to a hydrogel sample by their thickness-stiffness (bottom and left axes), which was fabricated using the recipe noted on the top and right axes (precursor volume (μL) versus PEG concentration (wt%)). All PEG hydrogels were immobilized on glass slides.

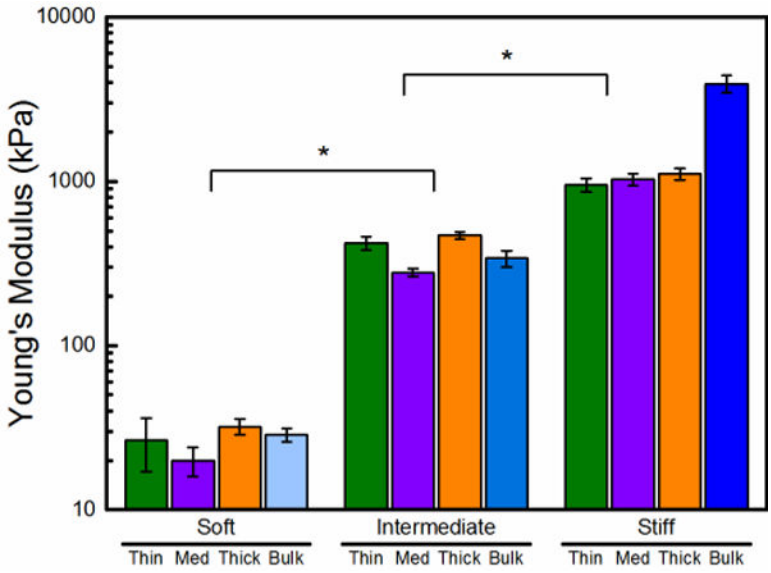

Figure 2.

The Young's modulus of PEG hydrogels increased with increasing polymer concentration. AFM nanoindentation and bulk rheology were used to determine the Young's modulus of soft (11 wt% PEG), intermediate (29 wt% PEG), and stiff (55 wt% PEG) hydrogels. Error bars denote standard error. An asterisk (*) denotes 99% significance between stiffness regimes.

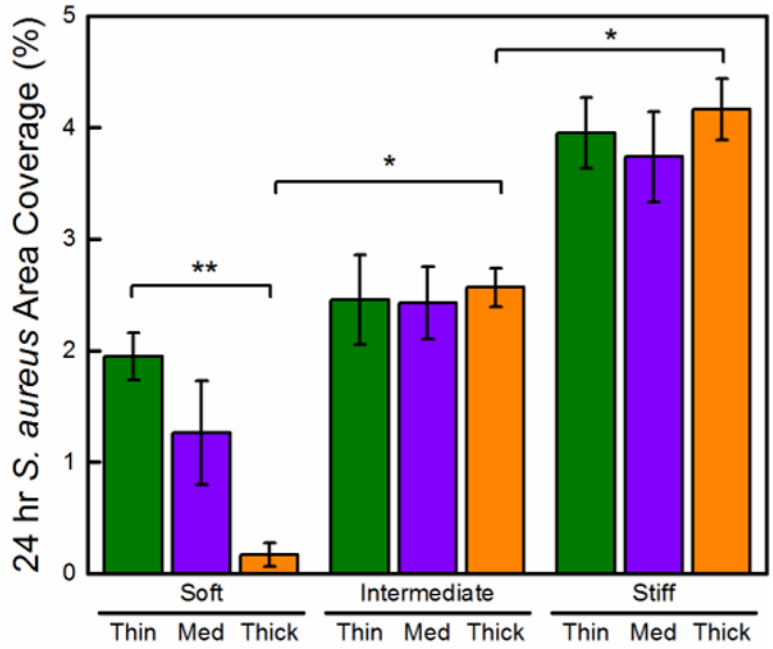

Figure 3.

S. aureus attachment is influenced by the thickness of soft hydrogels. The total *S. aureus* area coverage after a 24 h incubation period on thin (15 μm), medium (40 μm), and thick (150 μm) PEG hydrogels that were soft (30 kPa), intermediate (400 kPa), and stiff (1000 kPa). One asterisk (*) denotes 95% significance between hydrogels in different stiffness regimes. Two asterisks (**) denote 95% significance between samples of the same stiffness.

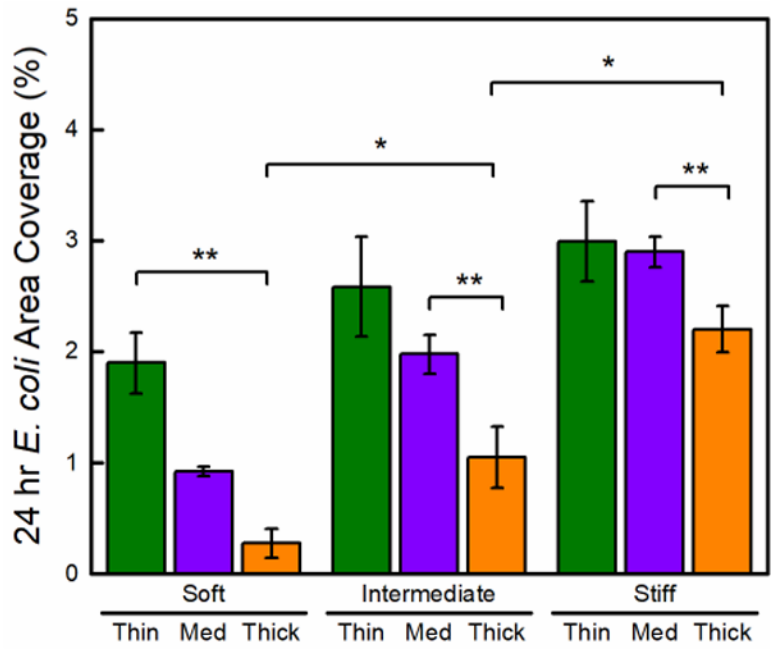

Figure 4.

E. coli attachment increased on thin hydrogels at all Young's moduli. Total *E. coli* area coverage after a 24 h incubation period on thin (15 μm), medium (40 μm), and thick (150 μm) PEG hydrogels that were soft (30 kPa), intermediate (400 kPa), and stiff (1000 kPa). One asterisk (*) denotes 95% significance between hydrogels in different stiffness regimes. Two asterisks (**) denote 95% significance between samples of the same stiffness.

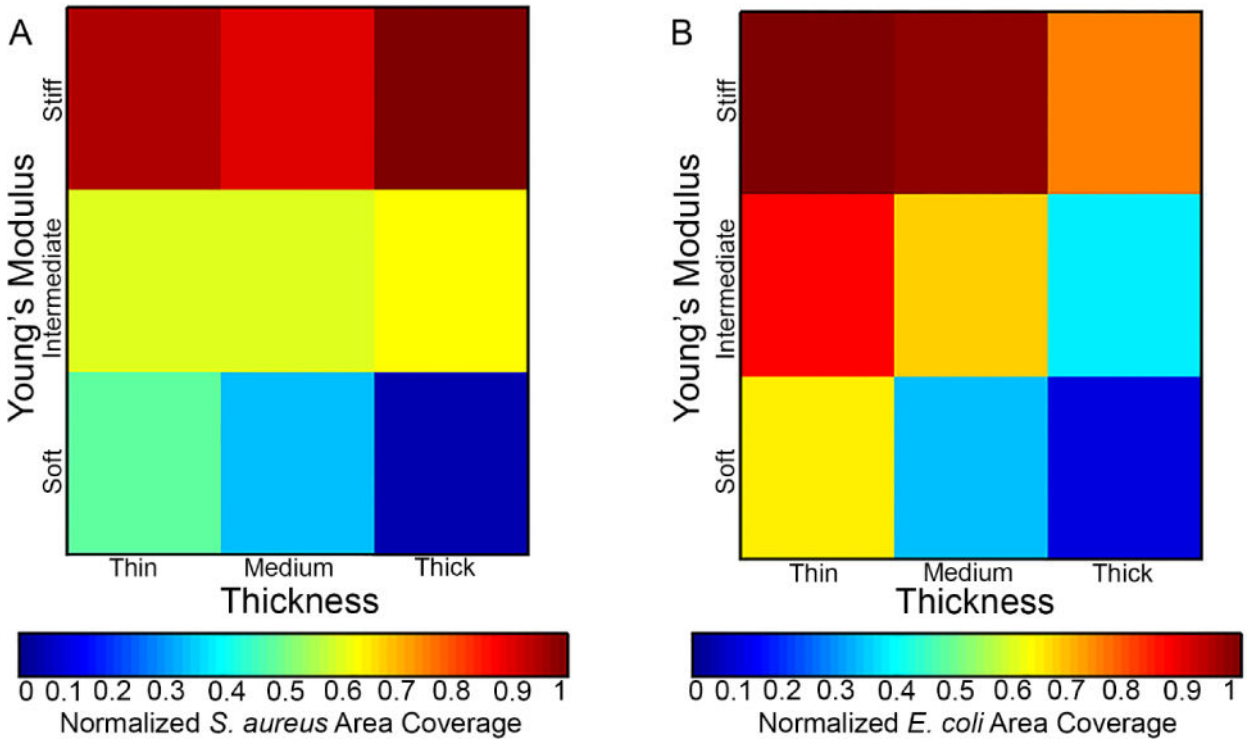

Figure 5.

Heat map displays of the normalized **(A)** *S. aureus* and **(B)** *E. coli* area coverage on hydrogels after a 24 h incubation period on thin (15 μm), medium (40 μm), and thick (150 μm) PEG hydrogels that were soft (30 kPa), intermediate (400 kPa), and stiff (1000 kPa). Data from Figures 3 and 4.